Polymer Journal (2017) 49, 245–254

www.nature.com/pj

ORIGINAL ARTICLE

Surface ionic charge dependence on the molecular mobility and self-assembly behavior of ionomers produced from carboxylic acid-terminated dendrimers

Thomas Chaffraix, Andreea S Voda, Ludovic F Dumée and Kevin Magniez

Dendrimers are unique molecular structures terminated by a multitude of peripheral functional groups that are accessible for targeted chemistry. Carboxyl-terminated dendrimers are attractive because their surface charge can be tuned, thus providing a highly versatile template for producing a range of ionomers with tailored properties. Here, a carboxylic acid-terminated dendrimer was synthesized from Boltorn, an aliphatic polyether polyol dendrimer, via a Steglich esterification with a succinic anhydride. A series of ionic dendrimers were subsequently produced by progressively neutralizing between 4 and 16 of the terminal carboxylic acid groups with sodium hydroxide, yielding their corresponding carboxylate sodium salts. With progressive neutralization, anion–cation electrostatic interactions in the ionic clusters dramatically affected the polymer chains' mobility, resulting in large increases in the order–disorder transition temperature. This result was substantiated with small angle X-ray scattering data, suggesting that the size of the ionic clusters increased from 2.2 to 3.8 nm as a result of long-range electrostatic interactions and core stretching. Self-assembly behavior in aqueous media into a large, 2D, tree-like morphology was demonstrated, highlighting potential applications as a multifunctional semiconductor in the drug delivery, colloidal science, sensing and catalysis fields.
Polymer Journal (2017) **49,** 245–254; doi:10.1038/pj.2016.93; published online 19 October 2016

INTRODUCTION

Dendrimers and hyperbranched polymers are densely branched macromolecules of well-defined geometry, which have been used in important scientific and technological applications, such as drug delivery, sensors, catalysis and advanced materials, largely due to their unique molecular structure.[1,2] Hyperbranched polyols based on the 2-bis(hydroxymethyl)propanoic acid aliphatic building block have been a focus of scientific attention because of their non-toxicity and biodegradability, making them attractive for biological applications. These polyester dendrimers are comparatively simple and cost-effective to produce through a number of esterification methodologies discussed recently in the literature.[3] Boltorn is a commercially significant hyperbranched polymer which, thanks to its terminal hydroxyl groups, can be used for the development of functionalized advanced materials via esterification,[4,5] alkene hydrothiolation,[6] amination[7] reactions and click chemistry.[1]

The term ionomer describes a polymer containing a number of acid-bearing groups of which some have been neutralized, forming an ionic pair with a cation. Over the past 20 years, there has been considerable academic and industrial focus on ionomers, in particular because ion incorporation leads to a dramatic enhancement in optical, mechanical and thermal properties of these materials. Depending on the number of groups neutralized, the ionic content varies. Studies of the structure–property relationships of ionomers have grown rapidly since the 1980s, when the amount of ionic content was established as having a marked effect on the unique microstructure of the ionomers, consequently affecting physical and mechanical properties.[8] For many years, those studying the field of ionomers have largely focused on elucidating the structure–property relationships of ionomers containing polyethylene, polystyrene and polybutadiene backbones.[8] More recently, ionomers derived from polymers with a dendritic or hyperbranched nature have attracted scientific attention.[9–13] An important review by Stoddart *et al.*[14] describes catalysis application of metal ion based dendrimers, demonstrating that the catalytic activity per metallic center can be improved as the number of localized metallic centers is increased. The production of dendrimers with tunable surface charges has enabled technological developments in colloidal science, where the properties and stability of macromolecules and colloidal systems are highly affected by electrostatic interactions achievable via ion absorption and coordination.[15] Other applications for these materials include high capacity cation exchange and drug delivery.[16]

Dendrimers bearing terminal carboxylic groups offer a highly versatile platform for producing surface-charged dendrimers via selective neutralization of the acid groups. The methodologies for synthesizing these dendrimers typically involve basic hydrolysis of terminal ester groups,[17] which is difficult to control and does not offer a high degree of tailorability of surface charges. The investigation of simpler syntheses for dendrimers bearing terminal carboxylic groups is therefore a significant and topical research area to further expand their

Institute for Frontier Materials, Deakin University, Geelong, VIC, Australia
Correspondence: Dr K Magniez, Institute for Frontier Materials, Deakin University, 75 Pigdons Road, Waurn Ponds, 3216 Victoria, Australia.
E-mail: kevin.magniez@research.deakin.edu.au
Received 7 June 2016; revised 16 August 2016; accepted 17 August 2016; published online 19 October 2016

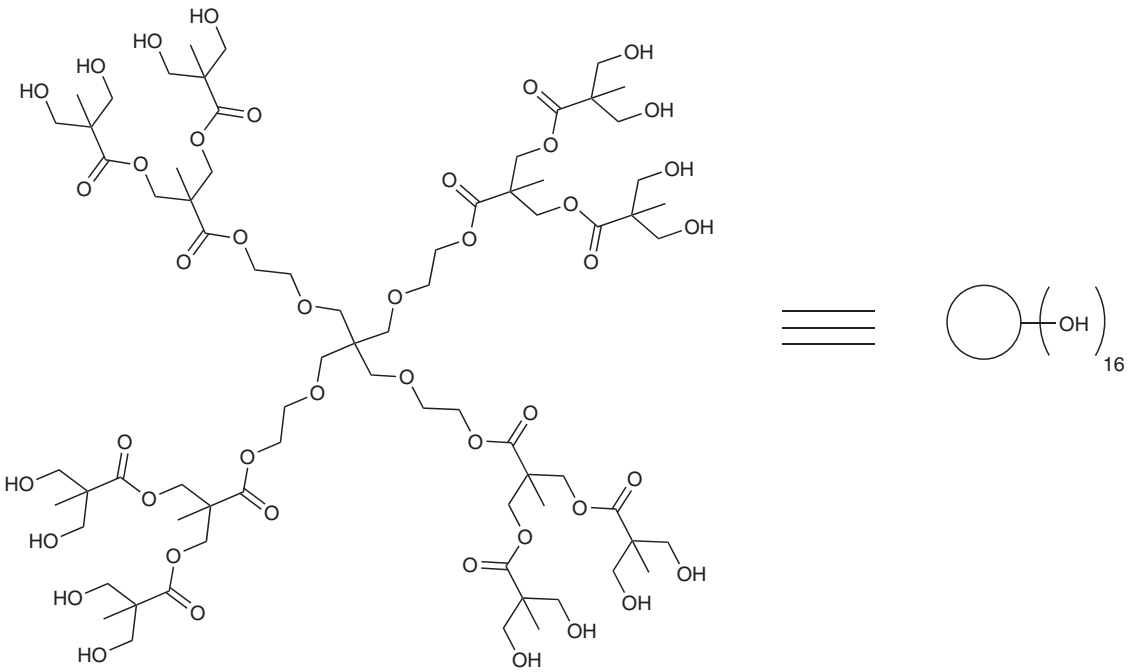

Figure 1 Polyol-terminated dendrimer (H_{20}) and its schematic representation.

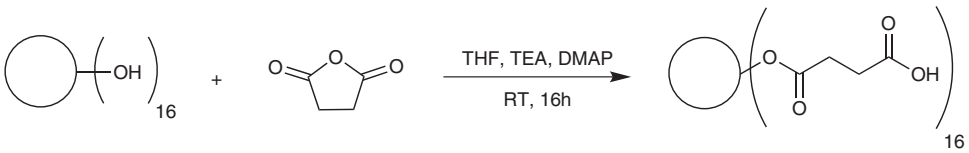

Scheme 1 Synthesis of H_{20}-COOH via Steglich esterification.

commercialization potential.[17] In this work, we report the functionalization of hyperbranched polyols (Boltorn) into a carboxylic acid-terminated counterpart, which will be used for the first time as a platform for producing a range of ionomers. The progressive conversion of the carboxyl groups into carboxylates was controlled via the addition of stoichiometric amounts of sodium hydroxide. The successful formation of ionic dendrimers having varying degrees of neutralization will be demonstrated, and their chemical and physical properties will be presented. Changes in the order–disorder transition temperature with progressive neutralization will be discussed, and self-assembly properties from aqueous milieu will be demonstrated, highlighting a potential application as multifunctional semiconductors.

MATERIALS AND METHODS

Materials

The starting material, a second-generation polyol-terminated dendrimer Boltorn (H_{20}), was sourced from Perstorp AB (Malmö, Sweden) and was used without further purification. The chemical structure of H_{20}, which contains a polyester core and is terminated with 16 hydroxyl groups, is displayed in Figure 1.

Synthesis and purification of the carboxylic acid-terminated dendrimer

To convert the terminal hydroxyls of the H_{20} dendrimer into carboxyl groups, a Steglich esterification was conducted in the presence of succinic anhydride, using triethylamine and 4-dimethylaminopyridine as the base and coupling agent, respectively (Scheme 1).[18,19]

The reaction was carried out using the Schlenk oxygen exclusion method in the presence of nitrogen. Typically, 0.50 g of vacuum-dried H_{20} (0.29 mmol) were dissolved in 10.0 ml of anhydrous tetrahydrofuran in a two-neck round-bottom flask, followed by the addition of an excess of succinic anhydride (0.55 g, 5.50 mmol) in the presence of 25 mg of 4-dimethylaminopyridine (0.20 mmol) and 5 ml of triethylamine. All additions were carried out under a nitrogen atmosphere, and the mixture was stirred at ambient temperatures overnight. During the reaction, a homogeneous and transparent solution formed initially, which then turned into a highly viscous solution. The final product was decanted to eliminate the tetrahydrofuran. The reaction compound H_{20}-COOH was washed three times with 20 ml of tetrahydrofuran and then three times with 20 ml of ethyl acetate to remove excess 4-dimethylaminopyridine. The purification was carried out via dialysis using a Thermo Fisher G2 2k cassette with a cutoff molecular weight of 2000 g mol^{-1}. The product H_{20}-COOH was mixed into 20 ml of purified water (Milli-Q) and dialyzed against 500 ml purified water for 14 consecutive days. The dialysis water was changed every other day and discarded.

During that time, the residual triethylamine ($M_W = 101.2$ g mol^{-1}), which is miscible with water, freely diffused across the dialysis membrane while product 2 (theoretical M_W of 3305 g mol^{-1}) remained trapped within the dialysis membrane. After dialysis, the product was taken from the dialysis membrane and analyzed with ^{1}H NMR in CD_3COCD_3 (Supplementary Figure S1), which demonstrated that the product was impurity free with no traces of triethylamine detected (quadruplet at 3.2 ppm and triplet at 1.3 p.p.m.). An average yield of 62% was obtained after reaction and purification. This carboxyl-terminated dendrimer was utilized for the preparation of various ionomers by

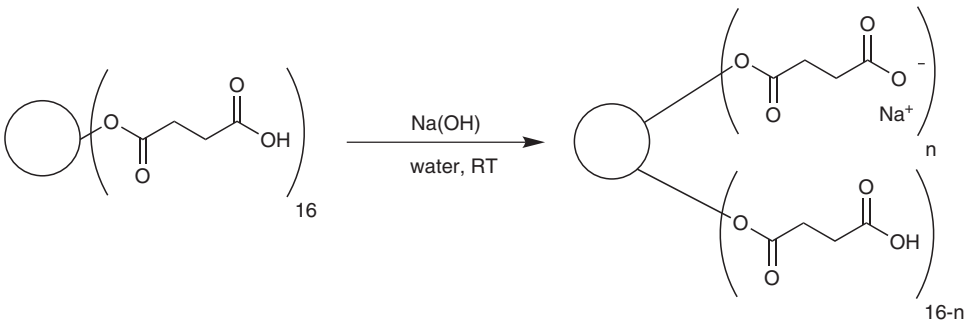

Scheme 2 Synthesis of the neutralized products H_{20}-COONa-1 ($n=4$), H_{20}-COONa-2 ($n=8$), H_{20}-COONa-3 ($n=12$) and H_{20}-COONa-4 ($n=16$).

neutralization of the carboxylic acid groups into the corresponding carboxylate salts.

General procedure for sodium neutralization

For the neutralization process, the following procedure was used. First, a 100 ml aqueous stock solution with a sodium hydroxide concentration of 0.25 mol l^{-1} was made by dissolving 250 mg of sodium hydroxide pellets (Puriss, >97%) into a vial with 100 ml of ultra-pure water (Milli-Q). The H_{20}-COOH dendrimer (1 g) was then dissolved in 20 ml purified water (Milli-Q) for 30 min. To this solution, stoichiometric amounts of the stock solution were added using a micropipette such that 4, 8, 12 or 16 of the carboxylic acid groups were converted to carboxylate groups with a corresponding sodium counterion (see Scheme 2). The neutralized products will be referred to throughout this paper as H_{20}-COONa-1 ($n=4$), H_{20}-COONa-2 ($n=8$), H_{20}-COONa-3 ($n=12$) and H_{20}-COONa-4 ($n=16$). To generate each of these products, 1 g of H_{20}-COOH was dissolved in 20 ml of purified water and stirred for 30 min followed by the addition of aqueous sodium hydroxide. The final solution was evaporated *in vacuo* at 60 °C for 4 h, yielding a thick paste used for sample processing.

Equipment and testing

Attenuated total reflectance. Infrared data were collected on a Bruker Vertex 70 FTIR equipped with an attenuated total reflectance accessory. The spectra were obtained in attenuated total reflectance mode from an average of 64 scans at a 4 cm^{-1} resolution between 600 and 4000 cm^{-1}. FTIR (ATR-diamond): ν (cm^{-1}) = 3600–3300 (b, H-bonded –OH carboxylic acid), 3300–2500 (st, free –OH carboxylic acid), 3000–2800 (st, CH_3/CH_2), 1735 (st, C=O ester), 1710 (st, C=O carboxylic acid), 1470 (b, C–H), 1300–1240 (st, C–O), 1220 (st, C–O carboxylic acid), 1040 (st, C–O ether), 960 (b, O–H carboxylic acid).

Nuclear magnetic resonance (NMR) spectroscopy. ^{1}H and ^{13}C NMR spectra were recorded on a Jeol 270 (at 270 and 100 MHz, respectively). All chemical shifts (δ) are reported in p.p.m. downfield of TMS. All spectra were recorded in a deuterated solvent ($CDCl_3$, D_2O or CD_3COCD_3) at 298 K. The NMR solutions were prepared at fixed concentrations of 5 mg ml^{-1} to avoid concentration shifts in the spectra.

^{1}H NMR spectra were acquired using 64 scans with a spectral window of 15 p.p.m., an acquisition time of 4 s and a relaxation time of 0.1 s. ^{13}C NMR spectra were acquired using an average of 50 000 scans with a spectral window of 250 p.p.m., an acquisition time of 1 s and a relaxation time of 0.1 s. Two-dimensional (2D) spectra were collected on a Bruker Advance 500 MHz spectrometer. All spectra were collected at room temperature using the residual proton resonance of the deuterated solvent as the internal standard. Proton signals are reported as chemical shift (p.p.m.) (integral, multiplicity (s=singlet, br s=broad singlet, d=doublet, dd=doublet of doublets, t=triplet and m=multiplet)) assignments.

^{1}H NMR (270 MHz, CD_3COCD_3); δ (p.p.m.) = 1.18–1.33 (m, 36H, CH_3), 2.54–2.56 (2 s, 80H, O $-CH_2-CH_2-$COOH), 3.42–3.76 (m, 16H, CH_2–O–CH_2 +R–CH_2OH), 4.14–4.39 (m, 56H, R–CH_2OR);

^{13}C NMR (100 MHz, CD_3COCD_3); δ (p.p.m.) = 17.17 (C7), 46.63 (C6), 48.54 (C1), 63.51 (C12), 64.22 (C13), 65.32 (C8), 65.74 (C4), 68.97 (C2), 70.65 (C3), 171.70 (C5), 173.25 (C14).

X-ray photoelectron spectroscopy (XPS). Survey spectra were acquired for binding energies of 0–1400 eV, using a pass energy of 160 eV. Chemical information indicating changes in the surface chemistry was elucidated by curve fitting the carbon 1 s peak (C1s). The spectra were fitted with a Lorentzian-Gaussian mix Voigt profile (SGL) function, using a nonlinear least squares curve fitting program (CasaXPS). The analysis areas for all the samples were 500 μm × 500 μm.

Differential scanning calorimetry. Thermal analyses were performed with a TA Instruments differential scanning calorimeter (Q200 model). Samples weighing approximately 5–10 mg were sealed in aluminum pans. The samples were first heated to 100 °C at a heating rate of 10 °C min^{-1} and held at that temperature for 5 min to erase any previous thermal history. The samples were then cooled to room temperature at a constant rate of 5 °C min^{-1} and heated again to 100 °C at a rate of 10 °C min^{-1}. The glass transition (T_g) was defined as the temperature at half the height of the shift in specific heat (C_p).

Dynamic light scattering. Dynamic light scattering measurements were collected on a Nanosizer ZS light scattering instrument (Malvern Instruments, Malvern, UK), equipped with a 4 mW He-Ne laser (emission 633 nm). The Nanosizer ZS employs non-invasive backscatter (NIBS) optics with a detection angle of 173°. The *z*-average diameter and the polydispersity index are measured by the instrument using cumulative analysis. For each measurement, approximately 1.5 mg of the compound was dissolved in 1.5 ml of Milli-Q water, and the solution was then passed through a 0.45 μm filter before being transferred into a polystyrene disposable cuvette for analysis.

Scanning electron images. Scanning electron micrographs of the fractal patterns and dendrimers were acquired on a JEOL 7800 scanning electron microscope (SEM). An accelerating voltage of 5 kV for a beam current of 11 μA was used with a working distance of 10 mm. The samples were deposited and dried onto silicon wafers and carbon-coated with a 1-nm-thick layer to reduce charging.

Determination of branch length was performed with image analysis software (GIMP) by measuring equivalent straight lines between nodes. Up to 75 arms were measured for statistical analysis. The average sizes of the 2D tree-like structures were also evaluated from SEM analysis by considering at least five patterns per measurement.

Small angle X-ray scattering. Small angle X-ray scattering (SAXS) data were acquired at the Australian Synchrotron on the SAXS/WAXS beamline using a 1.6 m camera length. The maximum q range was from 0.008 to 0.5 $Å^{-1}$. An in-vacuum undulator source (22 mm period, 3 m length maximum, K_{max} 1.56) at a beam energy of 11 keV was used. Tests were performed at 25 °C. The size distributions were evaluated with IRENA in the modeling II option for a unified fit model following a previously described method.[18] The form factor of the distribution was a spheroid of aspect ratio 1 with a dilute system structure factor. All fittings were performed across a narrow q range around the main diffraction peak.

RESULTS AND DISCUSSION

Esterification of the polyol dendrimer

The success of the esterification reaction between H_{20} and succinic anhydride, yielding the compound H_{20}-COOH, was collectively supported by the NMR, FTIR and XPS data. First, the infrared spectra of the starting material and the reaction compound (Figure 2) were found to correlate well with previously reported spectra.[19–21] The broad, strong band between 3600 and 3200 cm^{-1} visible in the H_{20} spectra results from the O–H stretch of the alcohol (Figure 2). The band between 3000 and 2800 cm^{-1} is characteristic of the C–H stretch present in the core of the molecule, while the strong band at 1735 cm^{-1} is very characteristic of the C=O ester stretch.[19] Another obvious characteristic band is at 1020 cm^{-1}, which is representative of the C–O–C ether stretching in the core.

Several distinctive bands suggest the formation of an ester bond between the terminal hydroxyl groups of H_{20} and the carboxyl group of succinic anhydride. In the fingerprint region, which is between 1400 and 800 cm^{-1}, the disappearance of the methylene stretch characteristic of the alcohol at 1045 cm^{-1} strongly indicates that all the alcohol functionalities have been grafted with succinic anhydride. In addition, a strong stretching band appears at 1170 cm^{-1} due to the C–O stretch of the carboxylic acid moiety (not to be confused with the C–O ester stretch at 1240 cm^{-1} or the C–O alcohol stretch at 1045 cm^{-1}). The broad absorption band between 3600 and 2500 cm^{-1} has been described as a combination of H-bonded carboxylic acid OH group vibrations (3600 to 3300 cm^{-1}), C–H alkyl group stretching (3000 to 2800 cm^{-1}) and free O–H group stretching (3300 to 2500 cm^{-1}).[21,22]

The ^1H NMR shifts for H_{20} and H_{20}-COOH are presented in Table 1. The ^1H NMR spectrum of H_{20} is supplied in the Supplementary Information in Supplementary Figure S2, while the ^1H NMR spectrum of the esterification product H_{20}-COOH is displayed in Figure 3. Table 1 also details the theoretical and experimental integration for each functional group present in both compounds. All proton integrations were normalized to the methyl groups (R–CH_3), which are the only constant moieties after

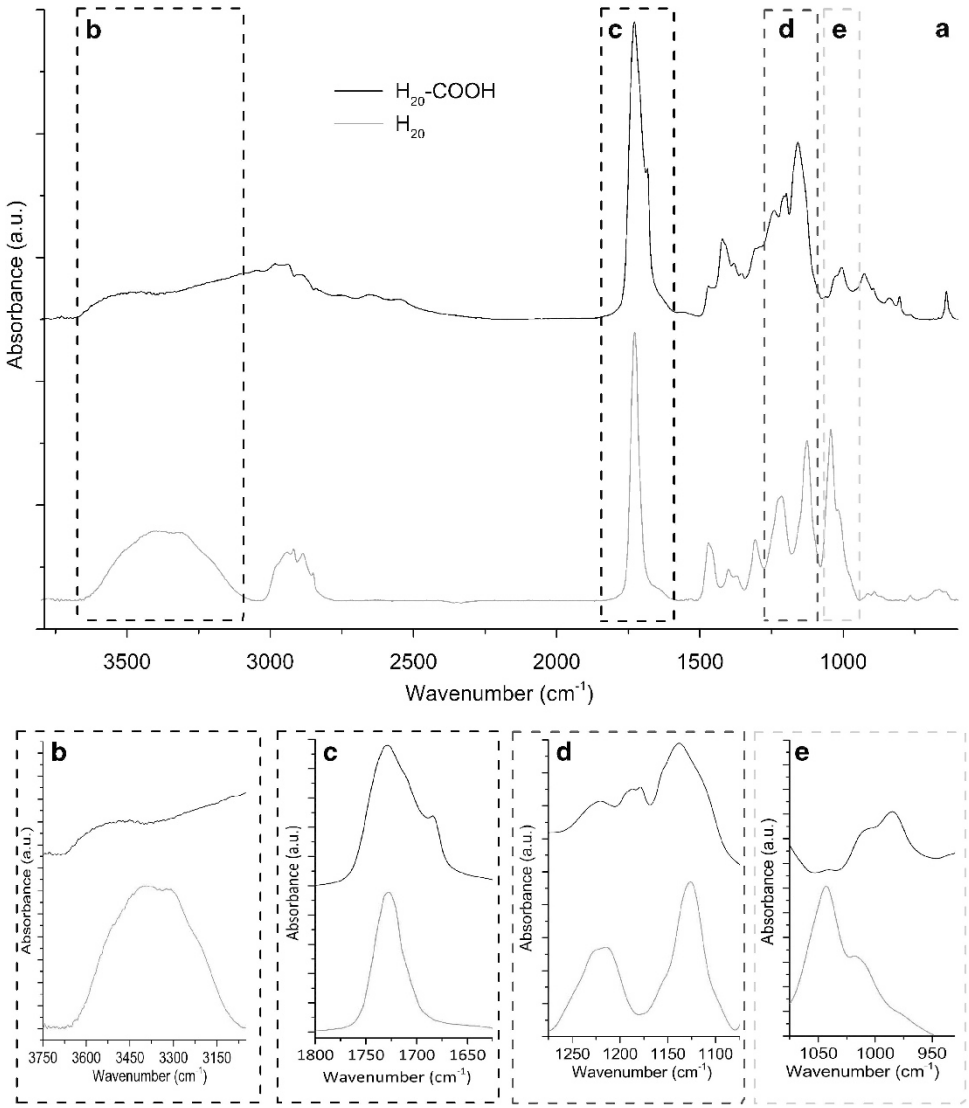

Figure 2 FTIR of H_{20} and the esterification product H_{20}-COOH (**a**) the hydroxyl region (**b**), carbonyl region (**c**), C–O stretch region between 1275 and 1075 cm^{-1} (**d**) and the C–O stretch region between 1075 and 925 cm^{-1} (**e**) have been highlighted for clarity. A full color version of this figure is available at *Polymer Journal* online.

Table 1 Theoretical (I_{th}) and experimental (I_{exp}) proton integration in H_{20} and H_{20}-COOH in CD_3COCD_3

	Carbon	*Functional groups*	δ *(ppm)*	I_{th}	I_{exp}
1	7, 10	R–C***H***$_3$	1.01–1.37	36	36.00
	2, 3, 11	R–C***H***$_2$ –R′ and R–C***H***$_2$OH	3.39–3.81	64	63.57
	4, 8	R–C***H***$_2$–OR′	3.98–4.40	24	23.92
2	7	R–C***H***$_3$	1.18–1.33	36	36.00
	12, 13	O–C***H***$_2$ –C***H***$_2$ –COOH	2.52–2.58	64	80.36
	2, 3	R–C***H***$_2$ –R′	3.42–3.76	16	16.53
	4, 8	R–*C**H***$_2$–OR′	4.14–4.39	56	55.33

Bold and italic entries indicate which protons are concerned by the integration.

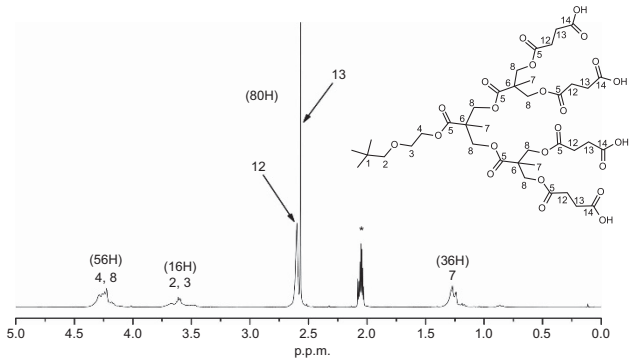

Figure 3 ^{1}H NMR of H_{20}-COOH in CD_3COCD_3 (* denotes the solvent peak). Note that because the dendrimer is symmetrical, only one branch is represented in the proton and carbon NMR shown here. The quaternary carbon in position 1 is representative of the molecular core.

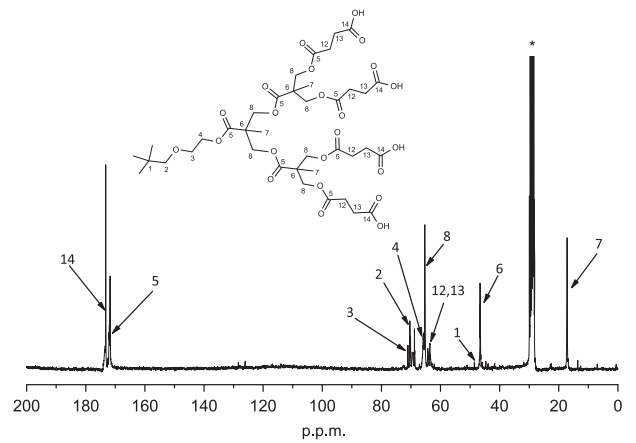

Figure 4 ^{13}C NMR of H_{20}-COOH in CD_3COCD_3 (* solvent peak).

esterification (36 protons). The ^{13}C NMR data of the starting material (Supplementary Figure S3) demonstrate the presence of quaternary carbon peaks in the 50 p.p.m. region. The peak at 48.7 p.p.m. represents the carbon at the dendrimer core (position 1), while the peak at 50.4 p.p.m. is the carbon shown in position 6 in Figure 3. In the CH_2 resonance region of the spectrum, which is between 60 and 75 p.p.m., the alkyl close to the ester groups (positions 8 and 4) can be observed at 65.2 p.p.m., and the two CH_2 groups of the ether (positions 2 and 3) are observed at 71.1 p.p.m. The carbons in the C=O ester groups (positions 5 and 9) resonate at 173.4 p.p.m.[23,24]

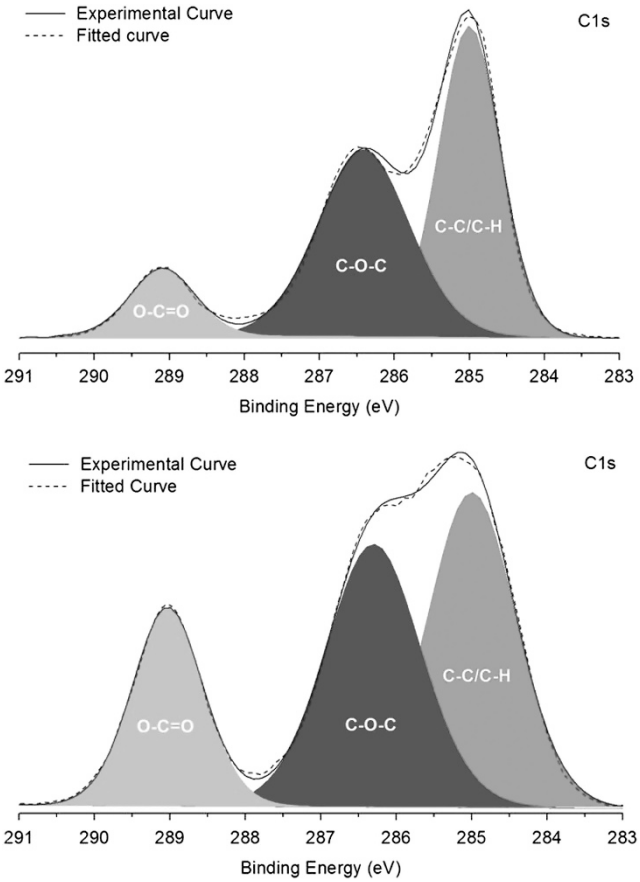

Figure 5 C1s XPS spectra of H_{20} (top) and H_{20}-COOH (bottom). A full color version of this figure is available at *Polymer Journal* online.

The ^{13}C NMR spectrum of H_{20}-COOH is displayed in Figure 4 and shows some critical differences compared with the starting material. The carbonyl region between 180 and 160 p.p.m. contains a distinct carbon peak at 173.3 p.p.m., characteristic of the carboxylic acid carbon (position 14) present in the grafted succinic acid. In the alkyl region (80–60 p.p.m.), the characteristic carbon peaks (positions 2 and 3) of the ether groups at the molecule's core are still present at approximately 71.1 p.p.m. Between 62 and 65 p.p.m., the ester group alkyl carbons (positions 4 and 8) at 66.3 p.p.m. remain, but the alcohol group alkyl carbon (position 10) at 64.6 p.p.m. disappeared after succinic anhydride attachment. The quaternary carbon (position 6) resonating at 46.5 p.p.m. displays a shift of 4 p.p.m. from its original position in H_{20} due to changes in the electronic environment after attachment. A similar trend was reported by Jesberger *et al.*[25] after grafting a RAFT agent on the surface of a hyperbranched polyester.

The elemental compositions of the compounds were investigated using XPS. The low-resolution, wide-scan XPS survey (Supplementary Information and Supplementary Figure S4) of both compounds primarily revealed the presence of carbon and oxygen elements. A large increase in the oxygen O1s peak (at 530 eV) in addition to the carbon 1s (C1s) peak (at 285 eV) was observed after the esterification reaction. The overall concentration of oxygen atoms (derived from the oxygen to carbon O/C ratio) nearly doubled after esterification, increasing from 1.03 for the starting material to 1.44 for its esterified product. The high-resolution C1s scans provided useful qualitative data relating to the carbon functional groups in each material. The C1s

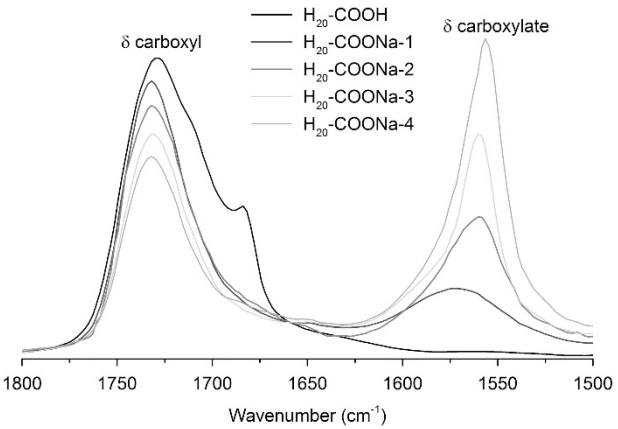

Figure 6 Changes in the carboxyl/carboxylate stretching bands in the 1500–1800 cm^{-1} region following neutralization with sodium hydroxide. A full color version of this figure is available at *Polymer Journal* online.

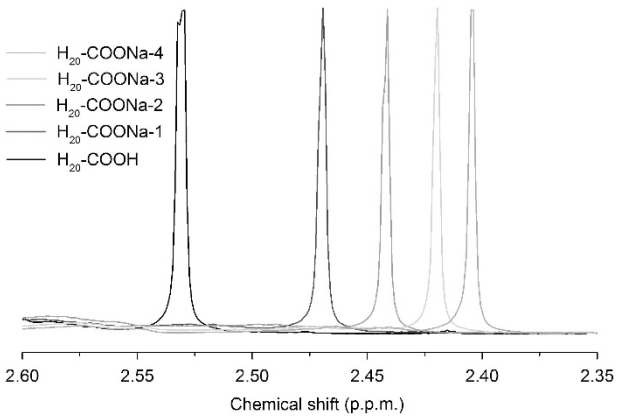

Figure 7 ^{1}H NMR shift in the CH_2 region of the various ionomers in D_2O. A full color version of this figure is available at *Polymer Journal* online.

peaks were deconvoluted, and curve fittings were performed to calculate the relative percent concentration of the functional groups (Figure 5).

A one-point manual normalization at 284.8 eV for the C1s line (C–C and C–H) was performed, and the three subpeaks at 285.0, 286.5 and 289.0 eV were assigned to C–C/C–H, C–O and O–C = O bonds, respectively, as reported elsewhere.[26,27] Supplementary Table S1 shows the elemental analysis of the different carbon binding energies. The C1s binding energies at 285 and 286.3 eV, corresponding to the C–C/C–H and C–O–C bonds, were found to decrease after esterification. This coincides with an overall decrease in the concentration of carbon bonds in comparison with oxygen bonds after succinic anhydride attachment. Concurrently, an increase was observed (10.9–21.1%) in the concentration of the O–C = O peak, corresponding to the ester and carboxyl moieties. Therefore, the FTIR, ^{1}H NMR, ^{13}C NMR and XPS data conclusively provide evidence that the carboxyl groups successfully attached at the original alcohol functionality.

Ionomer formation by progressive neutralization of the carboxylic acid terminal groups

The formation of ionomers, which was based on the progressive and selective neutralization of the carboxylic acid-terminated product H_{20}-COOH with sodium hydroxide, was carried out to better understand both the dependence of the number of surface ionic charges on the molecular mobility of these ionomers and the self-assembly properties of the ionomers. However, the neutralization procedure needed to be carried out with great precision to avoid de-esterification of the dendrimer core.[28] As shown in Supplementary Figure S5, a molar excess of sodium hydroxide as small as 10% led to the disappearance of the ester moieties in the corresponding ^{1}H NMR spectrum.

The effect of neutralization was clearly observed in the infrared spectra of the products (Figure 6), which revealed distinct changes in the carboxyl/carboxylate stretching bands in the 1500–1800 cm^{-1} region. The characteristic carboxylate band at 1555 cm^{-1} gradually increased in intensity with an increasing degree of neutralization. In contrast, the carboxylic acid band at 1735 cm^{-1} decreased (data were normalized at 1040 cm^{-1} corresponding to the C–O–C ether bond stretching vibration). This band, however, also overlaps with the core polyester stretching band, and, therefore, even after complete neutralization of the 16 carboxylic acid groups, an ester band at 1735 cm^{-1} remained. Furthermore, the single sharp band of the carboxylate group indicates a monovalent coordination with the sodium counterion.[29] The gradual increase in intensity of the carboxylate band at 1535 cm^{-1} also indicates a controlled neutralization. The weak shoulder at 1690 cm^{-1}, typical of the free OH bonding of carboxylic acid, was only present within the spectrum corresponding to the starting dendrimer; the shoulder disappeared upon ionomer formation. This is expected, as hydrogen bonding no longer exists after the carboxylic acid converts into a carboxylate group ionically bound to a sodium counterion.

As the infrared analysis results were merely qualitative, changes in the elemental composition of the carboxyl/carboxylate were quantitatively measured with high-resolution C1s XPS. An additional peak at 288.2 eV appeared in the C1s spectra of the neutralized products (H_{20}-$COONa^{-1}$ to Na-4), which has previously assigned to the carboxylate functionality (–O–C = O)[30,31] (see Supplementary Information and Supplementary Figure S5 for an illustrative example of C1s peak deconvolution for H_{20}-COONa-3). The atomic percent of the various carbon-related functionalities are tabulated in Supplementary Table S2.

The atomic ratios relative to the C–C/C–H (approximately 285 eV) and C–O–C (approximately 286.3 eV) binding energies were found to be relatively unchanged with respect to increasing neutralization, which was expected because this group is unaffected by the neutralization process. The integration of the –O–C = O peak also indicated an increase from 0.6 to 5.7% of carboxylate groups, while the O–C = O (ester and acid) peak area decreased from 20.4 to 14%. The experimental atomic percentage trends correspond well with the theoretical calculated prediction of atomic percentages during neutralization (taking into consideration 88 C–C/C–H, 80 C–O and 44 O–C = O linkages).

The variations in elemental composition of carboxyl/carboxylate groups confirmed by IR and XPS analysis were also corroborated in the ^{1}H NMR chemical shift of the $–CH_2$ methylene group (position 13) next to the carboxylic acid functionality (Figure 7). A gradual shift of up to 0.13 p.p.m. of the two protons could be observed as a result of the progressive conversion of carboxylic acid to carboxylate groups. This shift can be attributed to changes in the surrounding electronic environment of the methylene group protons, as has been previously reported.[32] The NMR shifts were obtained on the sample after progressive addition of aqueous sodium hydroxide (0.1 M) so that any concentration effects of the dendrimer in D_2O can be neglected.[33] These NMR shifts were found to coincide with a gradual increase in

Table 2 Order–disorder transition temperatures of the carboxylic dendrimer and its ionomers

Compounds	T_{g1} (°C)	T_{g2} (°C)
H_{20}-COOH	−16.6	x
H_{20}-COONa-1	−15.2	22.1
H_{20}-COONa-2	−14.7	31.9
H_{20}-COONa-3	−15.7	35.3
H_{20}-COONa-4	−14.5	43.9

pH from 4.5 and 5.9, suggesting that the neutralization was taking place in solution (Supplementary Figure S6).

Order–disorder transition of the ionomers

Polymers respond to temperature changes by undergoing a number of thermal transitions such as melting, crystallization and an order–disorder transition, often referred to as the glass transition. The order–disorder transition temperature, defined as the temperature at which the crystalline phase will evolve into an amorphous rubbery phase, is a property that is influenced by the ionic character of the polymer. Knowledge about this thermal order–disorder transition is an important consideration for polymer applications, as this transition directly correlates to changes in physical and mechanical properties.[33–35] In this work, the order–disorder transition temperatures of the various ionomers formed were investigated by differential scanning calorimetry.

First, the starting carboxylic acid dendrimer displayed a sub-zero glass transition temperature (T_{g1}) to the amorphous phase, which may also be referred to as a non-ionic amorphous phase, as the starting carboxylic acid dendrimer possesses no ionic character. As shown in the trends presented in Table 2, the mobility of this non-ionic amorphous phase was not affected by the neutralization process, considering that the corresponding glass transition T_{g1} remained relatively unchanged (between − 14.5 and 16.5 °C).

With progressive neutralization, a secondary order–disorder transition temperature (T_{g2}) associated with the transition of a phase-separated ionic amorphous phase[39] was observed. As the carboxylic acid to carboxylate group conversion progressed, T_{g2} was found to increase significantly by approximately 20 °C, from 22.1 to 43.9 °C. This result implies that the mobility of the chains is increasingly restricted as the ionic content increases, which agrees with the solid state ionomer morphology model reported by Eisenburg, Hird, and Moore (EHM).[36] In the EHM model, it is postulated that the ion–counterion and ion pair–ion pair associations regroup into discrete regions known as multiplets, the smallest form of an ionic aggregate.[37] At higher ionic concentrations, ionic clusters, defined as a group of several multiplets, will form locally ion-rich domains of size >20 Å.[38] The order–disorder transition temperature in ionomers has been found to be correlated to the degree of ionization because both the number and strength of the anion–cation electrostatic interactions in the clusters drastically affect chain mobility.[39]

SAXS data provided the most significant evidence of the extent of ionic aggregation in the sample. A sharp peak in the SAXS data at 0.12 $Å^{-1}$ was found to both shift towards a lower q range and intensify upon neutralization (Figure 8, top). In the starting carboxylic acid dendrimer, the peak observed at 0.12 $Å^{-1}$ corresponds to the scattering of the unimolecular dendrimer sphere.[40,41] The size of the equivalent sphere was estimated by modeling the data with Irena for an approximately spherical distribution. The model was found to fit the data extremely well for the reference dendrimer, while larger but modest traces (Supplementary Figure S7) were obtained for different levels of

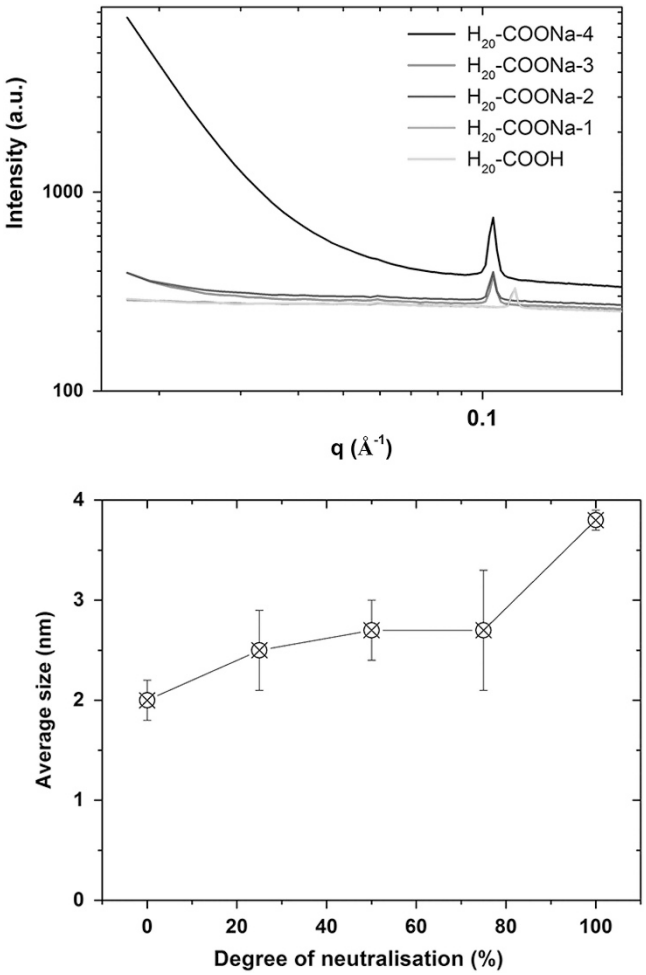

Figure 8 Reduced small angle X-ray scattering data corresponding to H_{20}-COOH and its ionomers (top) and the average modeled size of the spherical particles (bottom). A full color version of this figure is available at *Polymer Journal* online.

neutralization, which was in line with the slightly broader distributions obtained. Specifically, the average size of the modeled spheres was found to be approximately 2 nm, consistent with SAXS data previously reported by Prosa *et al.*[40] on the same hyperbranched polymer.

Upon neutralization, the estimated diameters of the ionic clusters (Figure 8, bottom) increased from 2.5 nm at 25% neutralization to 3.8 nm for the fully neutralized sample, which corresponds to the range of ionic cluster sizes previously reported in polyethylene-methacrylate ionomers.[39,42,43] Notably, the increase in cluster size did not occur gradually but rather in two stages. For a degree of neutralization below 75%, the ionic cluster size increased moderately to a size of approximately 2.8 nm; however, full neutralization induced a sharp increase in size (to approximately 3.8 nm). The reasons for this particular trend are still unclear. Nevertheless, we suggest that the size increment could possibly be attributed to long-range electrostatic interactions (i.e., Na ion pair dipoles and counterion condensation)[44] and core stretching as a result of surface charge localization.[45] The latter effect was, for example, reported during surface ionization of generations 4, 5 and 6 PAMAM dendrimers.[46] The intrinsic nature of the branched molecule and its associated steric hindrance may prevent any two aggregates from being closer than 3.8 nm center to center,[38] thus preventing extensive overlap of the ionic domains.

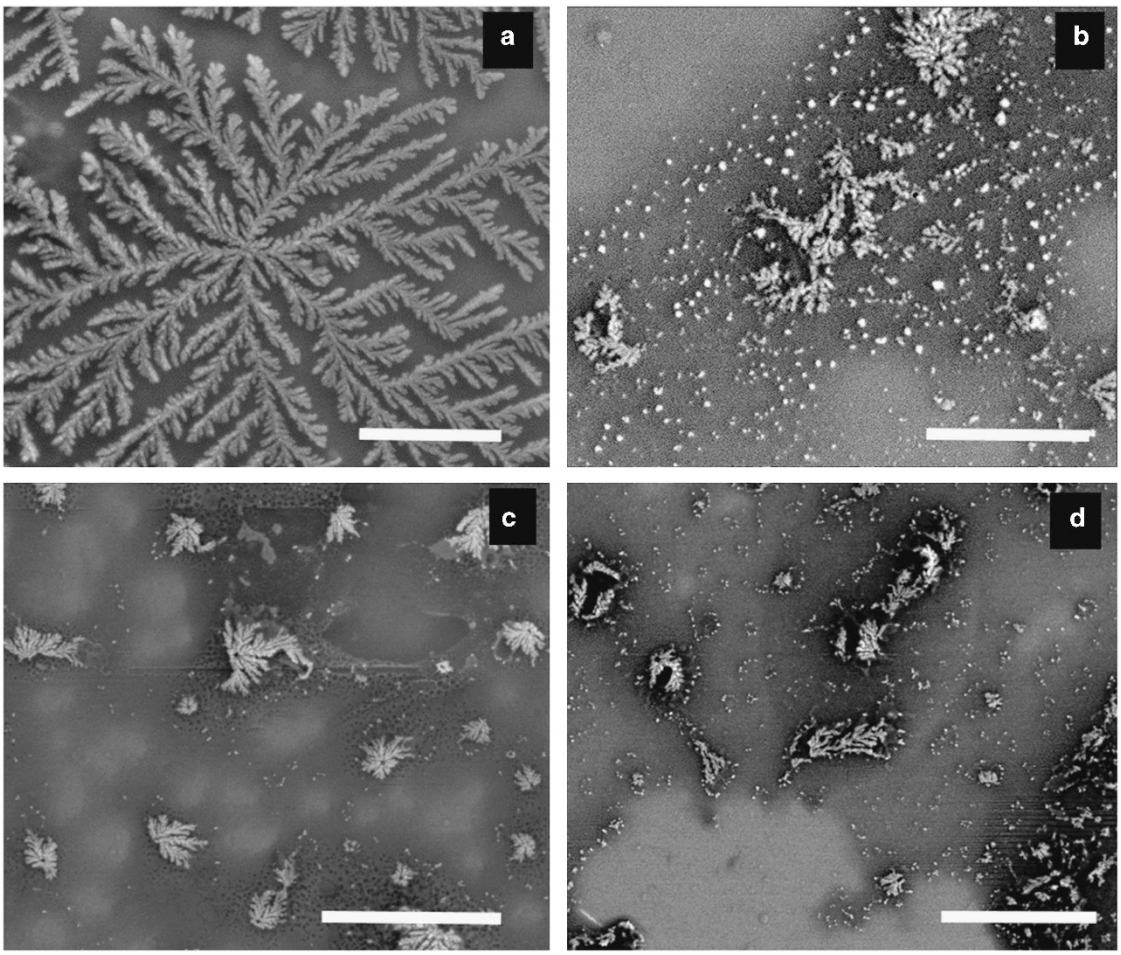

Figure 9 SEM image of an aqueous solution of H_{20}-*COOH* (**a**), H_{20}-*COONa2* (**b**), H_{20}-*COONa3* (**c**) and H_{20}-*COONa4* (**d**) deposited onto a silicon wafer. The scale bars correspond to 10 μm.

Self-assembly characteristics

The morphology of the carboxylic acid-terminated dendrimer and its corresponding ionomers is examined by scanning electron microscopy (SEM). The aim of this study was to determine the size and shape of the dendrimers produced as a function of the degree of conversion. Figure 9 shows the self-assembled carboxylic acid-terminated dendrimers into 2D tree-like morphologies larger than 20 μm. Higher magnification images also revealed the presence of constitutive self-assembled micelles of approximately 150–250 nm in size (Supplementary Figure S8), which is consistent with the range of hydrodynamic radii Rh of this compound measured by dynamic light scattering in aqueous milieu (Supplementary Figure S9 and Supplementary Table S3). The formation of thermodynamically stable self-assemblies can be attributed to hydrogen bonding interactions between micelles of the free hydroxyls on the carboxylic acid groups, as previously discussed by Eisenberg *et al.*[36,37]

The impact of neutralization on the self-assembly behavior of the various ionomers can be observed in Figure 9. Partially self-assembled tree-like structures were formed; the changes in geometrical parameters upon neutralization (number of branches and branch length) were analyzed from a series of SEM images, and the results are displayed in Figure 10. The results suggest that the neutralization process induced a drastic reduction in the size of the self-assembled structures, which may be attributed to the disruption of hydrogen bonding interactions and the increase of inter-molecular electrostatic interactions between the sodium counterion and the carboxylate upon neutralization. This is corroborated by the dynamic light scattering data of the dissolved compounds in aqueous milieu (Supplementary Figure S10), where the average hydrodynamic radius R_h was found to

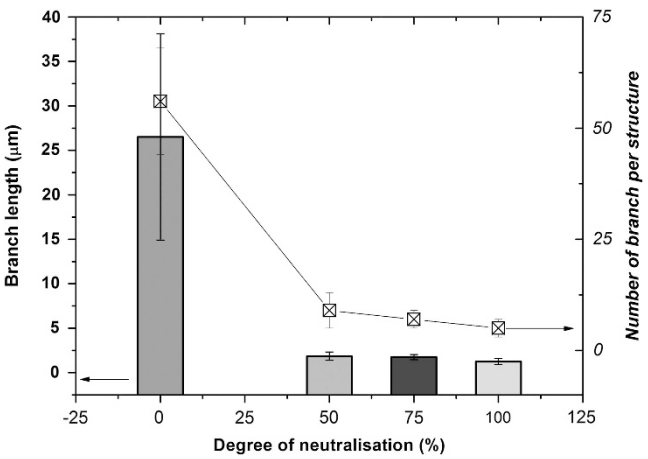

Figure 10 Geometrical parameter changes of the self-assembled tree-like morphologies as a function of the degree of neutralization. A full color version of this figure is available at *Polymer Journal* online.

increase with increasing neutralization, thus highlighting that the electrostatic inter-molecular interactions between the sodium counter-ion and the carboxylate must increase, resulting in larger aggregates. Regardless of these favorable electrostatic interactions, incomplete self-assembly between micelles was observed. The SEM images revealed that the partially formed tree-like structures are surrounded with aggregated micelles of a few hundred nanometers, which obviously did not participate in the self-assembly process. It is highly probable that the conditions were inadequate for complete self-assembly, and further investigation is needed to optimize electrostatic interactions and promote self-assembly. This phenomenon has been emphasized in the literature, and crucial factors, including polymer composition, concentration, solvent, temperature, the presence of counterions and relative humidity, have been shown to affect the self-assembly mechanism of ionomers based on hyperbranched polyesters.[47] Nevertheless, the partially self-assembled structures are highly organized, well-defined and large in size (several microns) and could still potentially be useful for multifunctional semiconductors[48–50] due to the existence of metallic ions within the 2D tree-like structures.

CONCLUSIONS

This paper reported the functionalization of a commercial, polyol dendrimer (Boltorn) into a carboxylic acid-terminated counterpart via a Steglich esterification with succinic anhydride. This carboxylic acid-terminated dendrimer was then used for the first time as a platform to produce a range of ionomers by progressive neutralization of the terminal carboxylic acid groups with sodium hydroxide. A wide range of spectroscopic data was used to confirm successful formation. We found that the degree of surface ionization influenced the molecular mobility of the polymer chains and that the order–disorder transition temperatures associated with the ionic cluster domains were above room temperature, up to approximately 44 °C. We also demonstrated that these materials self-assemble into micelles and that the electrostatic inter-molecular interactions between micelles led to the formation of 2D, tree-like morphologies. This characteristic in particular is very interesting as it suggests that these materials could be potentially useful for a number of applications. First, because of the existence of locally rich metal ions within the 2D tree-like structures, these structures may be useful as multifunctional semiconductors and in catalysis applications. Second, some ionomers display a transition near physiological temperatures. This is an important requirement for any polymeric drug delivery system because the slow-release mechanism of many drugs involves the careful tailoring of the polymer glass transition near physiological temperatures.[51] We therefore suggest that these materials could be potentially useful for the design of dendrimer-based drug delivery systems where dendrimer/drug ionic interactions are of great importance.[52,53]

CONFLICT OF INTEREST

The authors declare no conflict of interest.

ACKNOWLEDGEMENTS

The Advanced Manufacturing CRC is acknowledged for its financial support of this research project. We acknowledge the Australian Synchrotron, Adrian Hawley, Stephen Mudie and Nigel Kirby for fun, help and advice during the beamtimes M6410 and M7069. The assistance of Luke Henderson is acknowledged. LFD also acknowledges Deakin University for his Alfred Deakin Post-Doctoral Fellowship (ADPDF 2015). We also thank Dr Mark Nave and Dr Andrew Sullivan for their support with Electron Microscopy at Deakin University.

1 Katritzky, A. R., song, Y., Sakhuja, R., Gyanda, R., Meher, N. K., Wang, L., Duran, R. S., Ciaramitaro, D. A. & Bedford, C. D. Synthesis of Boltorn 1,2,3-triazole dendrimers by click chemistry. *J. Polym. Sci. A: Polym. Chem.* **47**, 3748–3756 (2009).
2 Bazzicalupi, C., Bianchi, A., Giorgi, C., Gratteri, P., Mariani, P. & Valtancoli, B. Metal ion binding by a G-2 poly (ethylene imine) dendrimer. Ion-directed self-assembling of hierarchical mono- and two-dimensional nanostructured materials. *Inorg. Chem.* **52**, 2125–2137 (2013).
3 Twibanire, J. d. A. K. & Grindley, T. B. Polyester dendrimers. *Polymers* **4**, 794–879 (2012).
4 Asif, A., Huang, C. & Shi, W. Structure–property study of waterborne, polyurethane acrylate dispersions based on hyperbranched aliphatic polyester for UV-curable coatings. *Colloid Polym. Sci.* **283**, 200–208 (2004).
5 Asif, A. & Shi, W. Synthesis and properties of UV curable waterborne hyperbranched aliphatic polyester. *Eur. Polym. J.* **39**, 933–938 (2003).
6 Fu, Q., Cheng, L., Zhang, Y. & Shi, W. Preparation and reversible photo-crosslinking/photo-cleavage behavior of 4-methylcoumarin functionalized hyperbranched polyester. *Polymer* **49**, 4981–4988 (2008).
7 Reul, R., Nguyen, J. & Kissel, T. Amine-modified hyperbranched polyesters as non-toxic, biodegradable gene delivery systems. *Biomaterials* **30**, 5815–5824 (2009).
8 Lantman, C. W., MacKnight, W. J. & Lundberg, R. D. Structural properties of ionomers. *Annu. Rev. Mater. Sci.* **19**, 295–317 (1989).
9 Mokrini, A. & Acosta, J. L. New ion conducting systems based on star branched block copolymer. *Polymer* **42**, 8817–8824 (2001).
10 Xie, D., Park, J.-G. & Zhao, J. Synthesis and preparation of novel 4-arm star-shape poly (carboxylic acid)s for improved light-cured glass-ionomer cements. *Dent. Mater.* **23**, 395–403 (2007).
11 Zhao, J. & Xie, D. A novel hyperbranched poly(acrylic acid) for improved resin-modified glass-ionomer restoratives. *Dent. Mater.* **27**, 478–486 (2011).
12 Storey, R. F. & Shoemake, K. A. Multi-arm star-branched polyisobutylene ionomers. *Polym. Bull.* **39**, 393–397.
13 Duncan, A. J., Layman, J. M., Cashion, M. P., Leo, D. J. & Long, T. E. Oligomeric A2 +B3 synthesis of highly branched polysulfone ionomers: novel candidates for ionic polymer transducers. *Polym. Int.* **59**, 25–35 (2010).
14 Stoddart, F. J. & Welton, T. Metal-containing dendritic polymers. *Polyhedron* **18**, 3575–3591 (1999).
15 Huang, Q., Dubin, P., Moorefield, C. & Newkome, G. Counterion binding on charged spheres: effect of pH and ionic strength on the mobility of carboxyl-terminated dendrimers. *J. Phys. Chem. B* **104**, 898–904 (2000).
16 Newkome, G. R., Yao, Z., Baker, G. R. & Gupta, V. K. Micelles. Part 1. Cascade molecules: a new approach to micelles. A [27]-arborol. *J. Org. Chem.* **50**, 2003–2004 (1985).
17 Engel, R. Ionic dendrimers and related materials. *Adv. Dendr. Macromol.* **2**, 73–99 (1995).
18 Dumée, L. F., Feng, C., He, L., YI, Z., She, F., Peng, Z., Gao, W., Banos, C., Davies, J. B., Hawkins, S., Duke, M. C., Gray, S., Hodgson, P. D. & Kong, L. Single step preparation of meso-porous and reduced graphene oxide by gamma-ray irradiation in gaseous phase. *Carbon* **70**, 313–318 (2014).
19 Zagar, E. & Grdadolnik, J. An infrared spectroscopic study of H-bond network in hyperbranched polyester polyol. *J. Mol. Struct.* **658**, 143–152 (2003).
20 Neises, B. & Steglich, W. Simple method for the esterification of carboxylic acids. *Angew. Chem. Int. Ed.* **17**, 522–524 (1978).
21 Bratož, S., Hadži, D. & Sheppard, N. The infra-red absorption bands associated with the COOH and COOD groups in dimeric carboxylic acid—II: the region from 3700 to 1500 cm – 1. *Spectrochim. Acta* **8**, 249–261 (1956).
22 Griffiths, P. R. & De Haseth, J. A. in *Fourier Transform Infrared Spectrometry*, 2 edn (University of Chicago, John Wiley & Sons, 2007)
23 Karataeva, F. K., Rezepova, M. V., Kutyreva, M. P., Kutyrev, G. A. & Ulakhovich, N. A. Structure of hyper-branched polyester polyol BOLTORN H2O-COOH. NMR data. *Russ. J. Gen. Chem.* **80**, 1831–1835 (2010).
24 Žagar, E. & Žigon, M. Characterization of a commercial hyperbranched aliphatic polyester based on 2,2-Bis(methylol)propionic acid. *Macromolecules* **35**, 9913–9925 (2002).
25 Jesberger, M., Barner, L., Stenzel, M. H., Malmström, E., Davis, T. P. & Barner-Kowollik, C. Hyperbranched polymers as scaffolds for multifunctional reversible addition–fragmentation chain-transfer agents: a route to polystyrene-core-polyesters and polystyrene-block-poly(butyl acrylate)-core-polyesters. *J. Polym. Sci. A Polym. Chem.* **41**, 3847–3861 (2003).
26 Beamson, G. & Briggs, D. *High Resolution XPS of Organic Polymers: The Scienta ESCA300 Database* (Wiley, USA, 1992).
27 Miao, H., Cheng, L. & Shi, W. Fluorinated hyperbranched polyester acrylate used as an additive for UV curing coatings. *Progr. Org. Coatings* **65**, 71–76 (2009).
28 Theodorou, V., Skobridis, K., Tzakos, A. G. & Ragoussis, V. A simple method for the alkaline hydrolysis of esters. *Tetrahedron Lett.* **48**, 8230–8233 (2007).
29 Painter, P. C., Brozoski, B. A. & Coleman, M. M. FTIR studies of calcium and sodium ionomers derived from an ethylene–methacrylic acid copolymer. *J.Polym. Sci. Polym. Phys. Ed.* **20**, 1069–1080 (1982).
30 Fukuda, R., Yoshida, Y., Nakayama, Y., Okazaki, M., Inoue, S., Sano, H., Suzuki, K., Shintani, H. & Van Meerbeek, B. Bonding efficacy of polyalkenoic acids to hydroxyapatite, enamel and dentin. *Biomaterials* **24**, 1861–1867 (2003).

31 Yoshida, Y., Van Meerbeek, B., Nakayama, Y., Snauwaert, J., Hellemans, L., Lambrechts, P., Vanherle, G. & Wakasa, K. Evidence of chemical bonding at biomaterial-hard tissue interfaces. *J. Dent. Res.* **79**, 709–714 (2000).
32 Masař, J. B., Pospíšil, H., Pleštil, J., Tuzar, Z. & Kiselev, M. A. NMR and SANS Study of poly(methyl methacrylate)-block-poly(acrylic acid) micelles and their solubilization interactions with organic solubilizates in D2O. *Macromolecules* **29**, 7853–7858 (1996).
33 Wouters, M. E. L., Litvinov, V. M., Binsbergen, F. L., Goossens, J. G. P., van Duin, M. & Dikland, H. G. Morphology of ethylene – propylene copolymer based ionomers as studied by solid state NMR and small angle X-ray scattering in relation to some mechanical properties. *Macromolecules* **36**, 1147–1156 (2003).
34 Van Krevelen, D. W. & Te Nijenhuis, K. *Properties of Polymers: Their Correlation with Chemical Structure; Their Numerical Estimation and Prediction from Additive Group Contributions* (Elsevier, 2009).
35 Fall, R. *Puncture Reversal of Ethylene Ionomers – Mechanistic Studies*. Masters of Science in chemistry thesis, Mechanistic Virginia Polytechnic Institute (Blacksburg, Virginia, 2001).
36 Eisenberg, A., Hird, B. & Moore, R. A new multiplet-cluster model for the morphology of random ionomers. *Macromolecules* **23**, 4098–4107 (1990).
37 Eisenberg, A. & Kim, J.-S. *Introduction to Ionomers* (University of Michigan, USA, Wiley, 1998).
38 Yarusso, D. J. & Cooper, S. L. Microstructure of ionomers: interpretation of small-angle x-ray scattering data. *Macromolecules* **16**, 1871–1880 (1983).
39 Bazuin, C. G. & Eisenberg, A. Modification of polymer properties through ion incorporation. *Ind. Eng. Chem. Prod. Res. Dev.* **20**, 271–286 (1981).
40 Prosa, T. J., Bauer, B. J., Amis, E. J., Tomalia, D. A. & Scherrenberg, R. A SAXS study of the internal structure of dendritic polymer systems. *J. Polym. Sci. B Polym. Phys.* **35**, 2913–2924 (1997).
41 Gröhn, F., Bauer, B. J., Akpalu, Y. A., Jackson, C. L. & Amis, E. J. Dendrimer templates for the formation of gold nanoclusters. *Macromolecules* **33**, 6042–6050 (2000).
42 Macknight, W. J., Taggart, W. P. & Stein, R. S. A model for the structure of ionomers. *J. Polym. Sci. Polym. Symp.* **45**, 113–128 (1974).
43 Marx, C. L., Caulfield, D. F. & Cooper, S. L. Morphology of ionomers. *Macromolecules* **6**, 344–353 (1973).
44 Pearsall, S. K., Green, M. M. & Morawetz, H. Titration of poly(carboxylic acid)s in methanol solution. Polymer chain extension, ionization equilibria, and conformational mobility. *Macromolecules* **37**, 8773–8777 (2004).
45 Rietveld, I. B., Bouwman, W. G., Baars, M. W. & Heenan, R. K. Location of the outer shell and influence of pH on carboxylic acid-functionalized poly (propyleneimine) dendrimers. *Macromolecules* **34**, 8380–8383 (2001).
46 Maiti, P. K., Cagin, T., Lin, S.-T. & Goddard, W. A. Effect of solvent and pH on the structure of PAMAM dendrimers. *Macromolecules* **38**, 979–991 (2005).
47 Li, J., Zhang, D., Li, S., Xu, Z., Chen, S., Li, T., Zhang, J., Chen, S. & Zhang, A. 2D self-sssembly of an amido-ended hydrophilic hyperbranched polyester by copper ion induction. *Macromol. Chem. Phys.* **214**, 1724–1733 (2013).
48 Manners, I. Putting metals into polymers. *Science* **294**, 1664–1666 (2001).
49 Park, S., Lim, J.-H., Chung, S.-W. & Mirkin, C. A. Self-assembly of mesoscopic metal-polymer amphiphiles. *Science* **303**, 348–351 (2004).
50 Mezzenga, R., Ruokolainen, J., Fredrickson, G. H., Kramer, E. J., Moses, D., Heeger, A. J. & Ikkala, O. Templating organic semiconductors via self-assembly of polymer colloids. *Science* **299**, 1872–1874 (2003).
51 Liechty, W. B., Kryscio, D. R., Slaughter, B. V. & Peppas, N. A. Polymers for drug delivery systems. *Annu. Rev. Chem. Biomol. Eng.* **1**, 149–173 (2010).
52 D'Emanuele, A. & Attwood, D. Dendrimer–drug interactions. *Adv. Drug Deliv. Rev.* **57**, 2147–2162 (2005).
53 Maingi, V., Kumar, M. V. S. & Maiti, P. K. PAMAM dendrimer–drug interactions: effect of pH on the binding and release pattern. *J. Phys. Chem. B* **116**, 4370–4376 (2012).

Supplementary Information accompanies the paper on Polymer Journal website (http://www.nature.com/pj)